Image Mining for Modeling of Forest Fires From Meteosat Images

Rajasekar Umamaheshwaran, Wietske Bijker, and Alfred Stein

***Abstract*—Meteosat satellites with the Spinning Enhanced Visible and Infrared Imagery (SEVIRI) sensor onboard provide remote-sensing images nowadays every 15 min. This paper investigates and applies image-mining methods to make an optimal use of images. It develops a simple, time-efficient, and generic model to facilitate pattern discovery and analysis. The focus of this paper is to develop a model for monitoring and analyzing forest fires in space and time. As an illustration, a diurnal cycle of fire in Portugal on July 28, 2004 was analyzed. Kernel convolution characterized the hearth of the fire as an object in space. Objects were extracted and tracked over time automatically. The results thus obtained were used to make a linear model for fire behavior with respect to vegetation and wind characteristics as explanatory variables. This model may be useful for predicting hazards at an almost real-time basis. The research illustrates how image mining improves information extraction from the Meteosat SEVIRI images.**

***Index Terms*—Forest fires, image mining, Meteosat, Spinning Enhanced Visible and Infrared Imagery (SEVIRI) Portugal, space–time modeling.**

I. Introduction

REMOTE-SENSING images, which are routinely being collected every day, offer an unprecedented opportunity for predicting and understanding the behavior of the Earth's ecosystem. This is particularly the case if images are combined with ecosystem models [1]. Although repositories of images can be used for a variety of different purposes, it may be hard to analyze each image individually and to explore relations with preceding and succeeding images at varying time steps [2], [3]. Therefore, a need exists to address an automated analysis of accumulated remotely sensed images.

A recent development in spatial inventarization methods concerns spatial data mining [4]. This can be defined as "The analysis of (often large) observational data sets to find unsuspected relationships and to summarize the data in novel ways that are both understandable and useful to the data owners" [5]. Spatial image mining, based on data mining, is a promising new field, focusing on large amounts of different images collected at various moments in time. It differs from automated image processing, which deals with a single or a few images [6], as many more images need to be processed in order to retrieve hidden knowledge. Spatial and multiband characteristics make remote-sensing imageries different from the general category of data [7].

Environmental concern has led to increasing monitoring efforts and predicting of ecosystem changes [8]. A typical example concerns forest fires that impair biodiversity, influence climate on regional and global scales, and promote soil erosion. Several remote-sensing satellites are currently used for fire prediction, detection, monitoring, and assessment. A major constraint in monitoring the forest fires of Europe and the savanna fires of Africa is the lack of observation time. Satellites such as BIRD, which are specifically designed for this purpose, are polar orbiting, thus prohibiting continuous observation.

Fire detection is one of the potentials of the Meteosat Second Generation satellites MSG-1 and MSG-2. These satellites are primarily designed to continuously observe the Earth's full disk by applying the Spinning Enhanced Visible and Infrared Imagery (SEVIRI) sensor [9]. It observes regions of Europe and Africa every 15 min. SEVIRI has 12 channels: three in the visible and eight in the infrared part of the spectrum, plus one High Resolution Visible (HRV) channel. Spatial resolution ($> 3 \times 3$ km in Europe) is coarse. An advantage of these satellites is that fire dynamics can be studied along with weather data that are available as well on MSG-1 and MSG-2.

This paper explores the potential of spatial image mining for SEVIRI applied to high temporal fire monitoring. A forest fire occurring in Portugal on July 28, 2004 is taken as an illustration. Images along with additional data from the satellite and CORINE land-cover data are combined to better understand the fire and predict its behavior.

II. Image Mining and Fire

A. Image Mining

In this paper, forest-fire objects are analyzed with image mining. Image mining is a relatively new development focusing on extracting relevant information from large sets of remote-sensing images [10]–[13]. It is well illustrated in Fig. 1. On a series of images, an object of interest is identified, using a segmentation and classification procedure. Although in principle, unsupervised objects could be identified, we focus for the moment on well-known and identifiable objects. Such an object essentially occurs at multiple images, requiring a linking in the space–time domain. Next, modeling describes the object

Manuscript received January 27, 2006; revised May 23, 2006.

R. Umamaheshwaran was with the International Institute of Geo-Information Science and Earth Observation (ITC), Enschede, The Netherlands. He is now with Indiana State University, Terre Haute, IN 47809 USA (e-mail: rajasekar07942@itc.nl).

W. Bijker and A. Stein are with the International Institute for Geo-Information Science and Earth Observation, 7500 AA Enschede, The Netherlands (e-mail: bijker@itc.nl; stein@itc.nl).

Digital Object Identifier 10.1109/TGRS.2006.883460

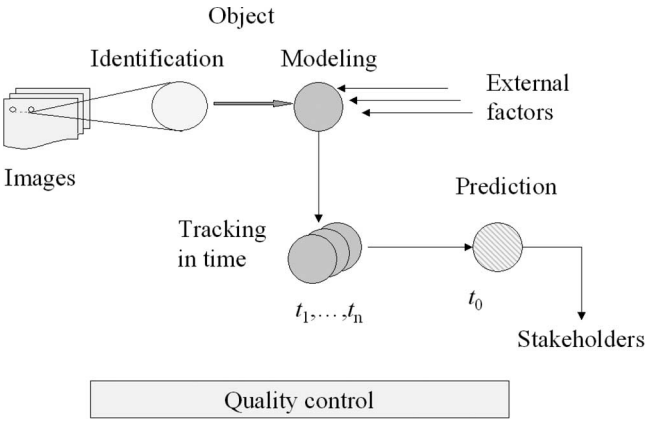

Fig. 1. Scheme of mining a series of images, from observation, through modeling, and tracking toward prediction.

with a function that relies on a limited set of parameters. Environmental and other external factors may be included. The object is then tracked in the space–time domain, and predictions are being made. Such a prediction may occur for a future time, for an intermediate time, or for the time before observation, e.g., to identify the start of a process. Predictions are then communicated to stakeholders.

In all steps, the issue of data quality is important. During identification, a precise description of the attributes and of the spatial coordinates and extent is to be done. During modeling, the appropriate scale and level of complexity are to be considered. Tracking and predicting both require care about the coordinates and their precision.

B. Remote Sensing and Fire

Several studies have been carried out in the past on remote sensing and fire. Lambin *et al.* [14] analyzed remotely sensed indicators of burning efficiency of savanna and forest fires. Giglio and Justice [15] in a study on wavelength, fire size, and temperature demonstrated that the location of 4- and 11-μm channels can cause large differences in fire temperatures for wildfires composed of both flaming and smoldering components. Mbow *et al.* [16] used spectral indexes and simulation of savanna burning to assess risk of intensive fire propagation within a national park.

Most satellites that are used for detection of fires and identification of their characteristics are not designed for hot-spot (fire) investigation. They are mainly polar-orbiting satellites and do not provide high temporal resolution images needed for active fire monitoring. Currently, only MSG-1 and MSG-2 can be used for continuous monitoring of fire in Europe and Africa. Their high time frequency of observation could help in characterizing the dynamic nature of forest fires.

Predicting the possible movement of a fire is important as a warning system for possible danger zones and in assisting fire fighters. Several models for studying the spread of fire have been proposed. Ameghino *et al.* [17] have developed a model based on cellular automata, including complex parameters. Muzy *et al.* [8] compared this with a comparable method across a fuel bed, concluding that it is more reliable and cost effective. Koutsias and Karteris [18] studied fuel complexes that favor fire occurrences and spread in the Mediterranean-type climate. They used Landsat Thematic Mapper and GIS layers to arrive at a relation between forest types and fire behavior.

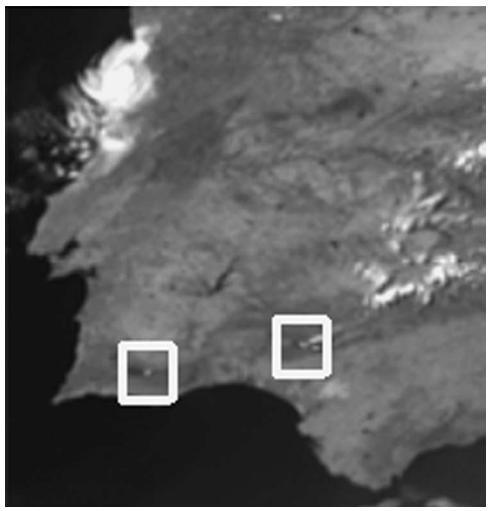

Fig. 2. Image acquired by Meteosat in visible bands (3, 2, 1) at 15:30 h. Square boxes show the area of active fires.

C. Study Area

The study area is located in the southern Algarve province in Portugal [9], [19], [20]. The area is regularly hit by fires [21]. A forest fire occurred in a central mountain area near the city of Loule (Fig. 2). It consisted of two large fires starting at night time, which merged into one large fire in the afternoon. In addition, four smaller fires were reported in the same region. The fires were detected with a fire-detection algorithm based on images from TERRA's and AQUA's MODIS sensors. The two large fires could be detected on SEVIRI images as well; the smaller fires could not be detected. Images were obtained on July 28, 2004. Preprocessing consisted of the conversion of images by means of geometric correction and corresponding radiometric corrections (to radiance in $\mathrm{mW/m^2/sr/(cm^{-1})^{-1}}$ for bands 1, 2, and 3 and to temperature in Kelvin for bands 4 to 11).

We applied SEVIRI for monitoring and analyzing the behavior of fire in space and time. Temporal resolution of SEVIRI is high, as in every 15 min, an image is recorded for all 12 channels simultaneously, resulting into 96 images per day. Owing to this high frequency, it is virtually impossible to analyze SEVIRI images manually, and mining methods are required. Spatial resolution is, however, low.

Data quality for remote-sensing imagery focuses on scale, the spectral resolution, and the radiometric resolution. Three issues are important when modeling forest fires from SEVIRI images.

1) Selection of the most suitable band. Studies by Cihlar *et al.* [9] and Giglio and Justice [15] show that fire can be detected by long wavelength bands, i.e., 3.9-μm band 4 of the SEVIRI sensor. Little work, however, has been done on identifying the relation between the type of fire and its thermal reflectance on this sensor.

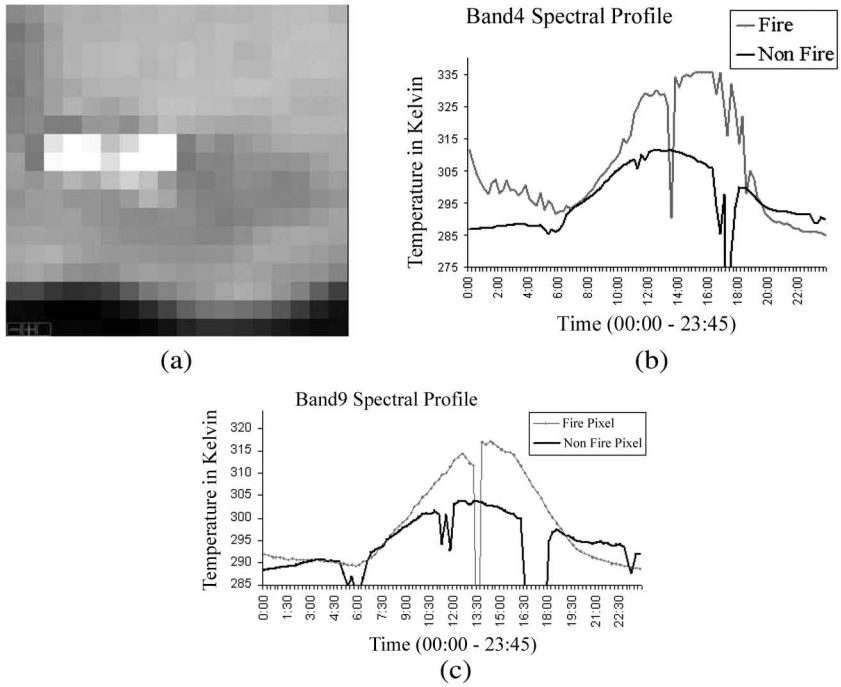

Fig. 3. Image (at 12:15 h) and spectral profile of band 4 for fire and nonfire areas (top) and spectral profile of band 9 (bottom).

2) The spatial resolution of the image, being equal to 3×3 km in the study area. If a fire is detected within a pixel, it is barely possible to identify its exact location, and spectral mixing likely occurs.
3) Validation of results. Detailed ground truth is commonly absent.

This paper focuses on the first two points—a proper validation was not possible.

III. Mining Fire From Meteosat Imageries

A. Band Selection

A subset of 18×18 pixels from SEVIRI images covering a region of approximately 54 km^2 was selected. Care was taken that the fire was well contained within this subset for its entire diurnal period. From the 12 bands, band 4 was selected in this paper. This band shows a bright white region in the middle denoting pixels with high temperature [Fig. 3(a)]. Band 4 also shows a profile during the 24 h of study that was clearly different from those observed without fire in the same area five days before [Fig. 3(b)]. A sudden drop in temperature during the early evening (around 18:00 h) is mainly due to the movement of fire from that pixel after burning. As the other bands are concerned: the visible bands (bands 1, 2, 3, and 12 = pan) are not suitable for fire monitoring, as no detectable signal could be observed during the night. This is a major drawback, as many fires start in the late afternoon [16], requiring a tracking during the night. Also, absorption bands 5 and 6 (water-vapor absorption bands), 8 (ozone absorption band), and 11 (carbon-dioxide absorption band) are not suitable for fire detection. This leaves bands 4, 7, 9, and 10 potential for fire monitoring. Spectral profiles of bands were analyzed to identify patterns. Saturation limits of band 4 (IR window of 3.9 μm), band 7 (IR window of 8.7 μm), and band 9 (IR window of 10.8 μm) were higher than those of the other bands. Band 4 showed better contrast between fire and background than for example band 9 (Fig. 3). Bands 7 and 10 were under the limit of saturation and would not give much information (not shown).

We focused on a single band, as addition of nonsuitable bands would add more noise than information. Further, an algorithm based on a single band is faster than one based on a combination of several bands. Speed is important in this type of fire monitoring. The algorithm is under development, however, and it can possibly be developed to work on a combination of bands.

B. Extraction of Fire Objects

Pattern analysis identifies or detects patterns from a given set of data using statistical or nonstatistical models by detecting and characterizing relations in the data [22]. To analyze the behavior of fire over a diurnal period, pixels with a thermal radiance higher than pixels in their neighborhood were identified as objects.

Fig. 4 shows the image subsets at three moments in time. The change in location of thermal activity represents fire movement. Regions under thermal activity are not clearly defined because of the low image resolution. No detection method is implemented for SEVIRI to separate fire pixels from nonfire pixels. To overcome this, we characterized fire pixels on the basis of a functional definition. First, we selected a suitable function to describe the characteristics of fire. Second, we described the patterns of variation over space using that function.

As thermal reflectance of one pixel is related to its neighboring pixels, a Gaussian bivariate function was selected for modeling. Two main considerations apply for this choice. First, heat dissemination by fire is continuous in nature. Therefore,

Fig. 4. Fire recognition during the diurnal cycle. (a) $t = 1$ (00:00 h). (b) $t = 49$ (12:15 h). (c) $t = 96$ (23:45 h). Bright white areas denote fire objects.

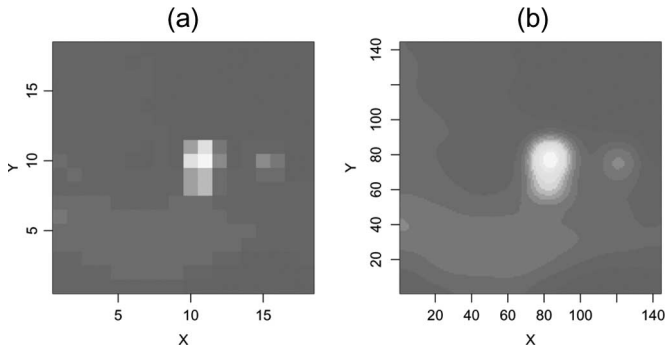

Fig. 5. Images (a) before and (b) after convolution.

the thermal reflectance of one pixel has influence on its neighboring pixels and vice versa. Second, this influence is Gaussian in nature, i.e., temperature is assumed to be transferred from one point to another gradually, and characteristics of this dissemination would be Gaussian with its peak at the center of the pixel. In addition, the rationale was to use a simple function for an effective and efficient characterization of the fire. For all these reasons, the Gaussian function is an appropriate choice. It is well adapted to represent both location and spread of fire in space and, hence, allows to both model track the fire objects. To each image $I(x, y)$, with x being the pixel location in the x direction and y the pixel location in the y direction, a Gaussian bivariate function was fitted, with its center as the center of pixels with maximum thermal radiance.

Splines, kernels [23], loess, and kernel convolutions [24] were explored to represent the data. We found that splines, kernels, and the kernel convolutions with the Gaussian function were best in this respect [22]. Further, kernel convolution was more efficient than the other methods [25]. Fig. 5 shows the subset image before and after convolution, using kernels to a lattice grid of 144 $\times$ 144. After some experimentation, we chose the smoothing parameters equal to $h = 0.20{-}0.25$ for the kernel convolutions based on [24], h equal to 8–10 times the image size for smoothing based on [23], and h equal to the image size for smoothing based on [25].

Kernel convolution was applied to all 96 images.

An algorithm was developed to automate this process using an ordinary least square fitting.

Once fitted, the function is subtracted from the main image leading to a residual image $I_{\text{sub}}(x, y)$ and a function $f(x, y)$. This process is summarized in the form of (1)

$$I_{\text{sub}}(x, y) = I(x, y) - hf(x, y) - c \tag{1}$$

where h is a scaling parameter, c is the global minimum of $I(x, y)$, and $f(x, y)$ is the Gaussian bivariate function, i.e.,

$$f(x, y) = \frac{1}{\sqrt{2\pi}\sigma_x\sigma_y} e^{-\frac{1}{2}\left(\left(\frac{x-\mu_x}{\sigma_x}\right)^2 - 2\frac{(x-\mu_x)(y-\mu_y)}{\sigma_x\sigma_y} + \left(\frac{y-\mu_y}{\sigma_y}\right)^2\right)}. \tag{2}$$

Here, μ_x and μ_y are the locations of the fire center, and σ_x and σ_y measure the extent of the fire into the x and y directions. This process is repeated n times, until no further maximum is identified that could signify a fire.

The final result equals

$$I_{\text{sub}}^{(n)} = I(x, y) - h^{(1)} f^{(1)}(x, y) - \cdots - h^{(n)} f^{(n)}(x, y) - c \tag{3}$$

where $h^{(n)}$ are the n scaling parameters, $f^{(n)}(x, y)$ equal the nth fitted functions with parameters $\sigma_x^{(n)}$, $\sigma_y^{(n)}$, $\mu_x^{(n)}$, and $\mu_y^{(n)}$, and $c = c^{(1)} + \cdots + c^{(n)}$ equals the sum of the minimum values after each iteration. Each function $f^{(i)}(x, y)$ represents an object that can be considered as a fire. The choice for the value of n is set heuristically equal to ten, as an image of the size of 54 km^2 unlikely covers more than ten fires, as identifiable from SEVIRI and as being relevant to fire fighting.

Fig. 6 shows the image before and after extraction of $n = 2$ fire objects. Fig. 6(d) shows the residuals after validating the left-hand side of the equation image: decomposition1 to its right-hand side. The root mean square of the error values were of the order of e^{-14}.

C. Tracking of Fire Objects

Extracted objects were tracked through time. Changes in intensity and splitting and merging of fire objects may occur rapidly (Fig. 7). Tracking of a fire object was based upon its location and the uncertainties σ_x and σ_y into the x and y directions. To relate an object at time t_i to an object at time t_{i+1}, we identified objects with the lowest distance in adjacent time frames, leading to connectivity of objects in time. An algorithm was developed for extracting n fires over each image, where n is the number of possible fires within any image. Fire behavior was analyzed for merging, corresponding to a reduction of the number of fire objects, splitting, i.e., an increase in the number of fire objects, and anomalies. An example of such an anomaly is an identified object of a sufficiently high temperature but with a too large distance to fires at the previous or the succeeding times to be realistic as a fire objects. Further, merging of fire objects could simply be handled. Splitting, however,

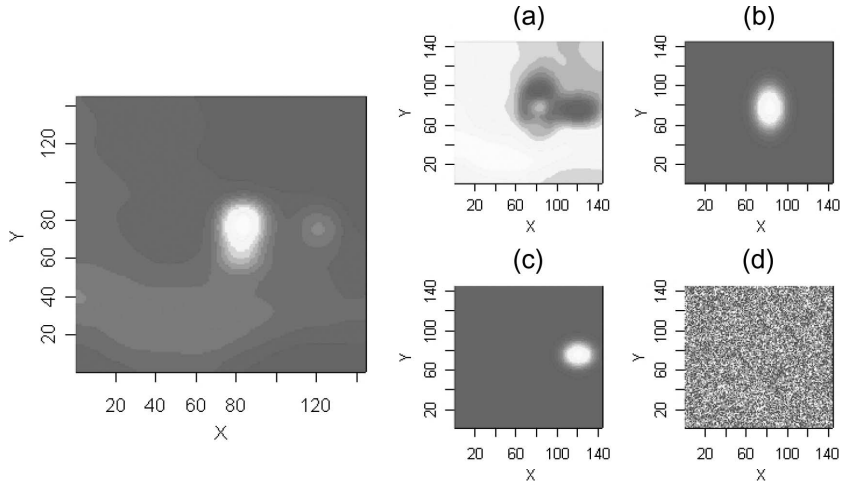

Fig. 6. Actual image (left) and its decomposition into (a) background, (b) and (c) two fire objects, and (d) residuals.

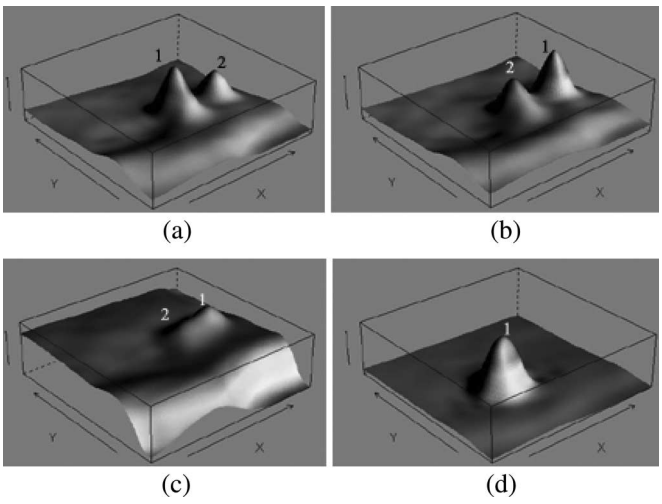

Fig. 7. Fire objects showing changes in intensity [from (a) to (b)] and merging of objects [from (b) through (c) to (d)].

complicated tracking, as it requires an initial starting point of the fire. We applied interactivity for this purpose using visual methods. To visualize and interpret fire behavior, we plotted the tracked objects in a space–time cube framework.

D. Space–Time Modeling

Patterns from the extracted and tracked objects represent empirical knowledge of location and characteristics of fire objects over time. These results were then used for further modeling the behavior of fire. To do so, we considered the following:

1) the direction of movement;
2) the effect of vegetation;
3) the weather conditions.

Vegetation patterns prior to fire were compared with the movement of fire. This was done using the normalized difference vegetation index (NDVI) data and land-cover data. NDVI data for time 12:30 h were generated from the SEVIRI images using the relation $\text{NDVI} = (\text{band } 2 - \text{band } 1)/(\text{band } 2 + \text{band } 1)$. Average NDVI values for July 23, 24, and 25 were taken to have reliable data. In addition, we used the 2000 Corine Land-Cover Data of the Iberian peninsula. Movement of the fire center was superimposed over these two vegetation sets.

TABLE I
ERROR OBTAINED FROM VARIOUS KERNEL-CONVOLUTION METHODS

Methods	RMSE
Kernel convolution based on [24] [26]	0.0981
Kernel convolution based on [23]	0.009
Kernel convolution based on [25]	0.0028

Weather conditions were included by considering wind direction and wind speed. Wind data were acquired from atmosphere motion vectors (AMV), a product of Meteosat (both first- and second-generation satellites). The AMV data, distributed in binary universal form for the representation of meteorological data (BUFR) format, were converted to text format. Then, based on time, location, spread, intensity, NDVI, wind direction, and wind speed at each time t, we developed a linear-regression model to predict the possible location of fire at time $t+4$, 1 h after observation as follows:

$$\hat{x}_{t+4} \sim \alpha_0 + \alpha_1 x_t + \alpha_2 \sigma_{x,t} + \alpha_3 I_t + \alpha_4 \text{WD}_t + \alpha_5 \text{WS}_t + \alpha_6 \text{NDVI} \quad (4)$$

$$\hat{y}_{t+4} \sim \beta_0 + \beta_1 x_t + \beta_2 \sigma_{x,t} + \beta_3 I_t + \beta_4 \text{WD}_t + \beta_5 \text{WS}_t + \beta_6 \text{NDVI}. \quad (5)$$

Here, x_t and y_t are the locations of the highest intensity in x and y directions, σ_x and σ_y are the spread in those directions, I_t is the intensity of the fire, WD_t is the wind direction in true degrees, and WS_t are the wind speed in Pascal all at time t, and NDVI is the vegetation index. Coefficients α_i and β_j are estimated from the data. The weighted sum was calculated using simple regression, with R^2 showing the importance of the model and its ability to use it for prediction.

IV. RESULTS

A. Characterizing Patterns Over Space

We first identified the best way of kernel fitting, comparing the Nadaraya–Watson smoother [24], [26], smoothing from [23] and from [25] (Table I). Methods using kernel

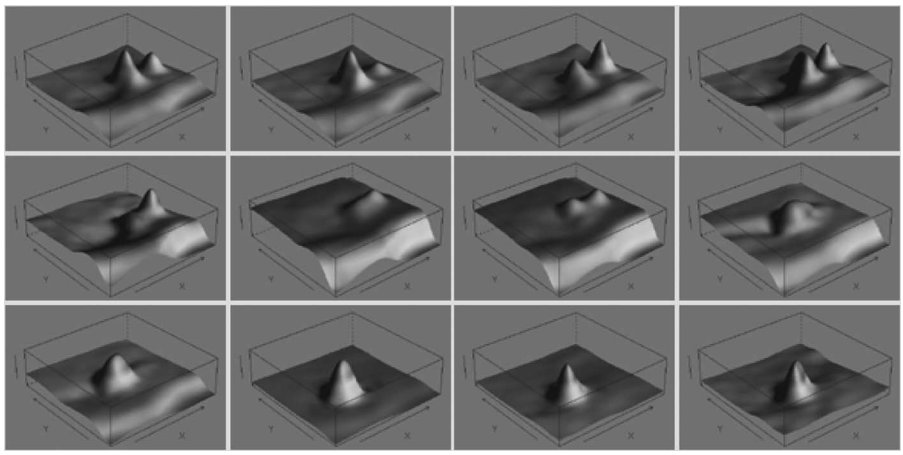

Fig. 8. Kernel convolution applied to a series of images. From top to bottom and left to right at times 00:00, 00:15, 02:30, 05:00, 07:30, 10:00, 12:30, 15:00, 17:30, 20:00, 22:30, and 23:45 h, respectively.

convolution perform relatively well. On the basis of the root-mean-square error (rmse) values, the smooth 2-D available from the fields library in R, which offers increased efficiency in processing by implementing the FFT was selected for characterizing the entire set of images.

Fig. 8 shows three-dimensional views of the kernel convolution applied to the series of images. Clearly, fire objects are characterized as Gaussian functions seen as peaks with respect to the background. From these images, we observe the following.

1) Background temperature slowly increases, reaching a maximum around noon (10:00–12:30) and then gradually decreases.
2) Fire objects change in intensity and in location with respect to time.
3) Two objects of fire are visible during the beginning of the day (00:00 h). These fires later merge into one fire (15:00 h).

The extraction algorithm characterizes fire objects on the basis of location centers and spread. Out of 960 originally extracted objects (ten objects at each time), 185 objects were tracked. From those, 103 objects were single objects, 61 objects were merging objects, and 21 were artifacts, respectively. Next, location centers were tracked over time based on their continuity and spatial correlation.

B. Space–Time Analysis

Fig. 9 illustrates the movement of fire in space and time. We observe that continuity is stronger for objects 1 and 2 than for object 3. Also, the swirling pattern of the fire objects in time is evident, which is caused by a combination of vegetation, wind, and topography.

Fig. 10 illustrates the movement of fire objects 1 and 2. Clustering of fire objects was observed during the early hours in the morning (around 08:00 h). This may be due to the building up of the fire, i.e., the attainment of a threshold before the fire starts moving. The figure also shows that objects 1 and 2

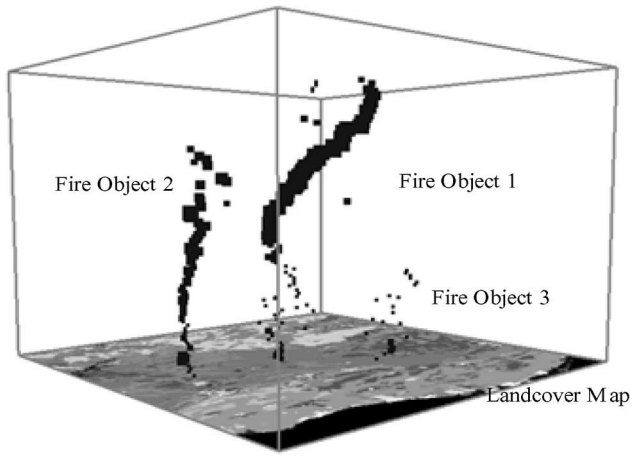

Fig. 9. Space–time cube showing the movement of fire in space and time. Size of an object is used as a visual variable for representing fire intensity.

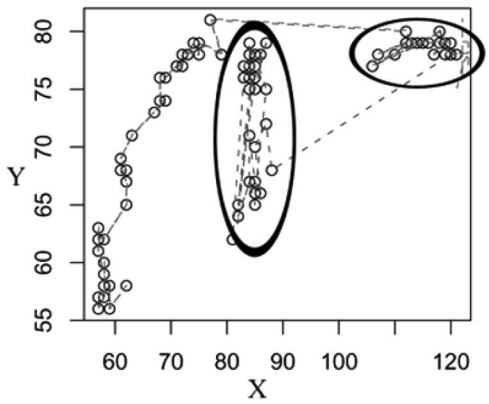

Fig. 10. Movement of fire objects in a 2-D plane. The ellipse delineates clustered fire objects.

are merging, as is represented by the dotted lines. Movement of the objects was stronger in the y direction than in the x direction.

Most of the area under fire had a relatively high NDVI value with a mean of 0.290 (see Table II). According to the

TABLE II
SUMMARY OF NDVI VALUES FOR THE LOCATION OF FIRE PIXELS

Total Number of fire objects	185
mean NDVI for those locations	0.290
Std.Dev of NDVI for those locations	0.014
min NDVI for those locations	0.262
First Quantile of NDVI for those locations	0.281
median	0.286
Third Quantile of NDVI for those locations	0.300
max NDVI from those locations	0.314
missing values	0.000

TABLE III
RESULTS OBTAINED FOR THE PREDICTION MODEL

i	$\alpha_i \pm$ std error	$\beta_i \pm$ std error
1	0.696 $\pm$ 0.047	-0.681 $\pm$ 0.056
2	0.320 $\pm$ 0.095	0.918 $\pm$ 0.123
3	69.461 $\pm$ 7.321	175.254 $\pm$ 6.972
4	-0.142 $\pm$ 1.16	-1.270 $\pm$ 1.693
5	-5.740 $\pm$ 8.265	-8.528 $\pm$ 12.379
6	47156 $\pm$ 9721	54027 $\pm$ 12161
0	-245305 $\pm$ 35585	1755344 $\pm$ 208311
R^2	0.975	0.942

classification by Williams [27], the fires were in the areas between medium and dense vegetation. Table II shows that 95% of the fire objects were in areas with relatively dense vegetation (NDVI ≥ 0.281 with the maximum of 0.314).

Out of 185 identified fire objects, 168 were within forest areas and 17 were in agricultural areas. Fire objects in agricultural areas were all artifacts.

C. Predicting the Motion of the Fire

Predictions were made for the possible movement of the fire within the next 1 h from the given instance n. The results obtained from the model are listed in Table III. Estimated α_1 and β_1 coefficients indicate that within the next hour, the fire likely moves some 700 m into the x direction and a similar distance into the negative y direction. A significant contribution of the uncertainty occurs as well, as is indicated by the α_2 and β_2 coefficients. Intensity contributes also to the spread, speeding it up into the x direction and slowing it down into the y direction. Wind size and speed did not have a significant influence on the spread of the fire, but vegetation as measured by the NDVI, was significantly influencing, with an emphasizing contribution into the x direction and a tempering contribution into the y direction.

R^2 values are high, showing the high predicting ability of the model.

V. DISCUSSION

We used band 4 for characterization of thermal activity over space. The key "active fire signal" is an increase of the observed radiance in the 3–5-μm region relative to the surrounding areas. The fire studied in this paper was well identifiable throughout its diurnal cycle. Other bands (7 and 9) were compared but did not show better performance. Description of the fire was done with the Gaussian bivariate function based on the nature of fire, the simplicity in description, and the behavior of heat in a vast area of land.

An exploratory analysis of various methods was done to find the best class of methods to describe the characteristics of the patterns within a single image. The kernel-convolution method was selected. It supports extension and reduction of dimensions. This can be helpful in extending this approach to define the patterns of variations for other phenomena that require more than one band to classify it over space.

Kernel convolution was applied to the actual image and image with normalized background. Normalization was done by subtracting the thermal radiance of the image acquired on July 28 with the mean thermal radiance of images acquired on July 23, 24, and 25 at corresponding times of the day. Results thus obtained were similar to those of the actual image, except that the background was exaggerated at early and late hours of the day and smoother during late morning and midday. Since these differences in radiance did not improve the model, the results from the actual image were considered for further modeling.

Extraction of fire objects was done by defining fire objects as being composed of a Gaussian bivariate distribution. It decomposed the image into a series of functions that separate fire objects from the background. It did result into some over- and underfitting of the fire objects but to a considerably less amount than for example characterizing rectangular regions of high thermal intensity (results not shown).

Tracking of fire objects might improve by including other attributes, such as volume, shape, and angle of objects at succeeding times. In addition, the simple differencing as we applied it might be improved, for example, by using the Kullback–Leibler distance or a probabilistic tracking approach. We did not expand upon this further in this paper in order to keep the model as parsimonious as possible and as tracking was already done sufficiently well. Further thought is to be given to make this algorithm more efficient.

The space–time analysis highlighted some aspects of utilization of the extracted knowledge. We focused on understanding the influence of wind, NDVI, and land cover. In the future, this can be used as well to study the influence of factors like topography, wetness index, and fuel index. Not surprisingly, we found that fire moved over the regions having high NDVI. Such modeling may be beneficial to predict the movement of fires as detected from SEVIRI images. Based upon the results of the model ($R^2 > 0.94$), we conclude that further research along this direction could lead to a further development of models to make even better predictions.

VI. CONCLUSION

This research aimed at developing a model from SEVIRI imagery for monitoring and analyzing the behavior of fire in space and time. To do so, we developed and applied methods from image mining. The developed mining model is promising in a case study from Portugal. We conclude that SEVIRI has a clear potential for giving rapid responses to track fires in a rapid way. It also provides meteorological data that were useful to better understand the behavior of forest fire.

REFERENCES

[1] D. Stockwell, "Improving ecological niche models by data mining large environmental datasets for surrogate models," *Ecol. Model.*, vol. 192, no. 1/2, pp. 188–196, 2006.

[2] S. Velickov, P. D. Solomatine, X. Yu, and K. R. Price, "Application of data mining techniques for remote sensing image analysis," in *Proc. 4th Int. Conf. Hydroinformatics*, 2000, [CD-ROM].

[3] Q. Ding, Q. Ding, and W. Perrizo, "Association rule mining on remotely sensed images using p-trees," in *Proc. 6th Pacific-Asia Conf. Advances Knowledge Discovery and Data Mining*, M. S. Chen, P. S. Yu, and B. Lu, Eds., 2002, pp. 66–79.

[4] V. Karasovâ, "Spatial data mining as a tool for improving geographical models," Masters thesis, Dept. Surveying, Helsinki Univ. Technol., France, 2005. (available in digital format).

[5] D. J. Hand, H. Mannila, and P. Smyth, *Principles of Data Mining*. Cambridge, MA: MIT Press, 2001.

[6] K. Koperski, G. B. Marchisio, and K. Meyer, "Information fusion and mining from satellite imagery and gis data," *Proc. 21st ESRI Int. User Conference*, 2002, [CD-ROM].

[7] S. Openshaw, "Geographical data mining: Key design issues," in *Proc. of the 4th Int. Conf. on Geocomputation*, 1999. (published in digital form). [Online]. Available: http://www.geovista.psu.edu/sites/geocomp99/Gc99/051/gc_051.htm

[8] A. Muzy, G. Wainer, E. Innocenti, A. Aiello, and J. Santucci, "Comparing simulation methods for fire spreading across a fuel bed," in *Proc. AIS—Simulation and Planning High Autonomy Systems*, 2002, pp. 219–224.

[9] J. Cihlar, A. Belward, and Y. Govaerts, *Meteosat Second Generation Opportunities for Land Surface Research and Application*, 1999, Hesse, Germany: EUMETSAT. Technical Document: EUMETSAT Scientific Publication EUM SP 01.

[10] P. Stanchev, "Using image mining for image retrieval," in *Proc. IASTED Conf. Comput. Sci. and Technol.*, Cancun, Mexico, 2003, pp. 214–218.

[11] S. Bajwa, P. Bajcsy, P. Groves, and L. Tian, "Hyperspectral image data mining for band selection in agricultural applications," *Trans. ASAE*, vol. 47, no. 3, pp. 895–907, 2004.

[12] J. Li and R. Narayanan, "Integrated spectral and spatial information mining in remote sensing imagery," *IEEE Trans. Geosci. Remote Sens.*, vol. 42, no. 3, pp. 673–685, Mar. 2004.

[13] H. Daschiel and M. Datcu, "Information mining in remote sensing image archives: System evaluation," *IEEE Trans. Geosci. Remote Sens.*, vol. 43, no. 1, pp. 188–199, Jan. 2005.

[14] E. F. Lambin, K. Goyvaerts, and C. Petit, "Remotely-sensed indicators of burning efficiency of savannah and forest fires," *Int. J. Remote Sens.*, vol. 24, no. 15, pp. 3105–3118, Aug. 2003.

[15] L. Giglio and C. O. Justice, "Effect of wavelength selection on wildfire characterization using the Dozier retrieval," *Int. J. Remote Sens.*, vol. 24, no. 17, pp. 3515–3520, 2003.

[16] C. Mbow, K. Goïta, and G. B. Bénié, "Spectral indices and fire behavior simulation for fire risk assessment in savanna ecosystems," *Remote Sens. Environ.*, vol. 91, no. 1, pp. 1–13, May 2004.

[17] J. Ameghino, A. Troccoli, and G. Wainer, *Models of Complex Physical Systems Using Cell-Devs*, 2001.

[18] N. Koutsias and M. Karteris, "Classification analyses of vegetation for delineating forest fire fuel complexes in a Mediterranean test site using satellite remote sensing and GIS," *Int. J. Remote Sens.*, vol. 24, no. 15, pp. 3093–3104, Aug. 2003.

[19] J. Schmetz, P. Pili, S. Tjemkes, D. Just, J. Kerkmann, S. Rota, and A. Ratier, "An introduction to meteosat second generation," *Bull. Amer. Meteol. Soc.*, vol. 83, no. 7, pp. 977–992, Jul. 2002.

[20] EUMETSAT, *The Meteosat Archive–User Handbook*, 2001. Technical Document EUM TD 06, EUMETSAT.

[21] J. M. C. Pereira and Y. Govaerts, *Potential Fire Applications From Msg/SEVIRI Observations*, 2001. Technical Memorandum No.7.

[22] J. Shawe-Taylor and N. Cristianini, *Kernel Methods for Pattern Analysis*. Cambridge, U.K.: Cambridge Univ. Press, 2004.

[23] A. W. Bowman and A. Azzalini, "Applied smoothing techniques for data analysis," in *Oxford Statistical Science Series*. New York: Oxford Univ. Press, 1997.

[24] E. A. Nadaraya, "On estimating regression," *Theory Probab. Appl.*, vol. 10, no. 1, pp. 186–190, 1964.

[25] D. Higdon, "Space and space–time modeling using process convolution," in *Quantitative Methods for Current Environmental Issues*, C. Anderson, V. Barnett, P. C. Chatwin, and A. H. El-Shaarawi, Eds. New York: Springer-Verlag, 2002, pp. 37–56.

[26] G. Watson, "Smooth regression analysis," *Shankya*, vol. 26, no. 4, pp. 359–372, 1964.

[27] J. Williams, "Geographic information from space," in *Processing and Applications of Geocoded Satellite Images*, ser. Wiley-Praxis Series in Remote Sensing. Chichester, U.K.: Wiley, 1995.

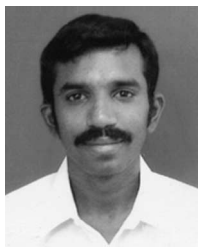

Rajasekar Umamaheshwaran received the engineering degree in civil and construction technology from the Center for Environmental Planning and Technology (CEPT University), Gujarat, India, and the M.Sc. degree in geoinformatics from the International Institute for Geo-Information Science and Earth Observation (ITC), Enschede, The Netherlands. He is currently working toward the Ph.D. degree at Indiana State University, Terre Haute.

He has worked as an Analyst and Spatial Solution Provider in India. His main research interests are in modeling, spatial data mining, geodatabases, and soft computing.

Wietske Bijker received the M.Sc. degree in soil science of the tropics and subtropics and the Ph.D. degree from Wageningen University, Wageningen, The Netherlands, for a study on the use of radar for rain-forest monitoring carried out at the International Institute for Geo-information Science and Earth Observation (ITC).

She is currently an Assistant Professor in remote sensing with the ITC, with special attention on monitoring, modeling, and land-cover mapping. Applications include both optical and radar remote-sensing data for monitoring of forests and crops.

Alfred Stein received the M.S. degree in mathematics and information science, with a specialization in applied statistics, from the Eindhoven University of Technology, Eindhoven, The Netherlands, and the Ph.D. in agricultural and environmental sciences from Wageningen University, Wageningen, The Netherlands.

He is currently a Professor of mathematical and statistical methods for geodata with the ITC International Institute for Geo-Information Science and Earth Observation, Enschede, The Netherlands, where he heads the department of Earth Observation Science. His main interest is in spatial statistics and data mining, including spatial data quality. Applications emerge from a range of agricultural, urban, and environmental fields. He is the Chief Editor of the *International Journal of Applied Earth Observation and Geoinformation*.